THE JOURNAL OF PHYSICAL CHEMISTRY C

ARTICLE

pubs.acs.org/JPCC

Systematic Tuning the Hydrodynamic Diameter of Uniformed Fluorescent Silica Nanoparticles

Gulay Durgun, Kasim Ocakoglu,† and Serdar Ozcelik*

Izmir Institute of Technology, Department of Chemistry, 35430 Urla, Izmir, Turkey

Supporting Information

ABSTRACT: We report a facile method for systematic tuning of the hydrodynamic diameter of uniformed fluorescent silica particles in the size range from 12 to 465 nm. Dynamic light scattering and electron microscopy studies demonstrate that the hydrodynamic size distribution of the silica particles is uniform. We show that the initial amount of ethanol and ammonia are essential to tune the size of these particles. The hydrodynamic diameter of such a particle increases as the amount of ammonia is increased. An increase in the amount of ethanol leads to the formation of smaller particles. A higher initial amount of ethanol yields an increase in the concentration of ethoxide ions and a decrease in the concentration of hydroxide ions. Such control over the concentration of hydroxide ion, which is responsible for the formation of siloxane bonds, causes a controlled-growth of the silica particles, resulting in precise tuning of the hydrodynamic size. We confirm that a linear relationship exists between the size and brightness of particles, demonstrating that the amount of dye molecules in such particles can be regulated by the presented method. We prove that the silica network provides protection for dye molecules encapsulated in particles against solvents, fluorescence quenchers, and unfavorable pH of environments. Moreover, the fluorescent silica particles with the size of 12, 50, and 250 nm were found to not be cytotoxic against the epithelial cell lines of MCF7 and PC3, even when the dosage levels up to 1.0 mg/mL and incubation periods up to 72 h were applied.

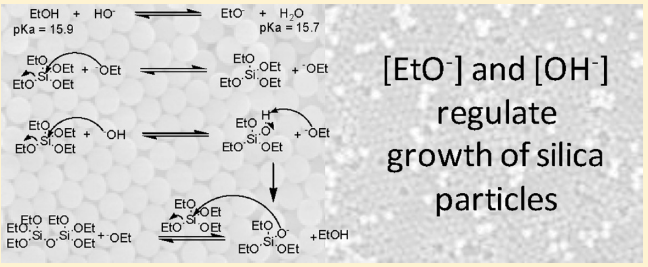

INTRODUCTION

Fluorescent silica nanoparticles are one of the preferred materials for labeling in bioanalysis and biotechnological applications. Their silica shell, shown to be biocompatible and nontoxic,[1] protects fluorescent dye molecules from the surrounding environment and encapsulates the dyes in its network,[2] providing photostability and signal enhancement, respectively.[3−12] Moreover, easy surface modification of silica promotes conjugation of biomolecules such as proteins, peptides, antibodies, oligonucleotides, and so on.[4,5,12−18] In general, two methods have been used for the synthesis of silica-based nanoparticles: the reverse microemulsion[19−25] and the Stöber method.[26] These methods offer certain advantages with some limitations. For instance, in the reverse microemulsion method, excellent uniformity of the particles on the nanometer scale can be obtained, and their surfaces are easily modified with functional groups including thiol, amine, and carboxylate during reaction.[19−25] Dye molecules can be released from silica matrix because of the lack of the covalent attachment of a fluorophore to the silica matrix, leading decreased brightness.[27,28] In addition, this method requires a large amount of surfactants and organic solvents. Alternatively, the method introduced by Stöber in 1968[26] is usually the choice for the preparation of pure silica particles and hydrophobic organic dye-doped particles.[29−33] This method is comparatively simple yet limited by the uniformity of particles, particularly those in the sub-50 nm range. Therefore, filtration and further separation techniques are usually applied to obtain particles with uniform size distribution. Additional silica coating (postcoating) with functional groups after particle synthesis is a way to modify surfaces of particles for specific applications.

Studies aiming at controlling particle size have been focused on how nanoparticle synthesis is affected by the relative amounts of reagents used;[16,29−33,39,44,47−52] however, diverse results regarding to control size were reported in the literature of silica particles. Yokoi et al. introduced a novel method to prepare particles in the presence of octane, water, and basic amino acids instead of ammonia under weakly basic conditions (pH 9 to 10). This new method produced highly monodisperse particles in the size range of 12−23 nm.[47,48] Recently, the formation mechanism of this new technique and the role of the amino acids, L-lysine and arginine, were explained.[49] In a similar study, successful control of the size of particles was achieved by Hartlen et al. by using arginine as the basic amino acid in the medium.[52]

The integration of fluorescent molecules into silica particles has been well studied.[27−42] Incorporating dyes into a silica matrix may be realized by covalent binding as well as via electrostatic interactions between the dye molecules and the silica matrix.[43,44] Van Blaaderen et al. introduced covalent binding of dye molecules into silica particles. Larson et al. synthesized particles with

Received: May 9, 2011
Revised: June 21, 2011
Published: July 28, 2011

dx.doi.org/10.1021/jp204323d | J. Phys. Chem. C 2011, 115, 16322–16332

Table 1. Experimental Conditions and Results of DLS Measurements - Hydrodynamic Diameter of Particles Measured under Various Experimental Conditions[a]

exp. no.	1[b]		2[c]		3[d]		4[e]	
reagents	ammonia		ethanol		TEOS		APTS-FITC	
	$[NH_3]$ (M)	D_{DLS} (nm)	[EtOH] (M)	D_{DLS} (nm)	[TEOS] (M)	D_{DLS} (nm)	vol (mL)	D_{DLS} (nm)
A	0.13	17 ± 2	11.4	465 ± 109	0.07	48 ± 6	0.060	32 ± 4
B	0.25	27 ± 6	13.7	255 ± 10	0.14	46 ± 7	0.100	38 ± 8
C	0.49	37 ± 2	14.7	105 ± 29	0.20	44 ± 2	0.160	22 ± 4
D	0.95	181 ± 50	15.2	48 ± 4	0.27	31 ± 6	0.320	28 ± 9
E	1.78	445 ± 76	15.8	31 ± 2	0.33	27 ± 9	0.640	36 ± 10
F			16.1	12 ± 4	0.39	26 ± 7		

[a] Standard deviations were determined from the size distributions. [b] Experiments were performed at room temperature in the presence of 0.1 mL of APTES-FITC, 1.2 mL of TEOS, 30 mL of ethanol, and 0.3−4.8 mL of ammonia. [c] Experiments were performed at room temperature in the presence of 0.1 mL of APTES-FITC, 1.2 mL of ammonia, 1.2 mL of TEOS, and 5.0−60 mL of ethanol. [d] Experiments were performed at room temperature in the presence of 0.1 mL of APTES-FITC, 1.2 mL of ammonia, 30 mL of ethanol, and 0.5−3.0 mL of TEOS. [e] Experiments were performed at room temperature in the presence of 1.2 mL of ammonia, 1.2 mL of TEOS, and 30 mL of ethanol.

three different architectures possessing the same size, ∼30 nm. They demonstrated that the brightness of the particles increased because of enhanced radiative rate. The Weisner group successfully improved their method and achieved preparation of fluorescent particles with hydrodynamic diameter as small as 6.6 nm.[45] They showed that silica particles circulate in the mouse body up to 6 h without the accumulation in organs such as liver and kidney. This study proves the possible utilization of silica nanoparticles for clinical applications. Ma et al. investigated the effects of interactions between dye molecules for the particles in the range from 15 to 200 nm and showed that the quantum yield of particles increased in the case of covalent bonding.[46] Hence, they recommend that dyes should be conjugated into a silica network by covalent bonding. Recently, Ha et al. initiated a new coupling method.[51] In this method, the consecutive allylation and hydrosilylation processes were applied to organic dyes to derivatize them. The new method aimed to eliminate the use of (3-aminopropyl) triethoxysilane (APTES), which otherwise causes agglomeration of particles. After the structure of the dye molecules was modified in two steps, the derivatives were conjugated into the silica matrix by the Stöber method. Additionally, they varied the size of particles from 30 to 500 nm by adjusting the concentration of TEOS, ammonia, and water. Relatively longer processing and purification times after allylation require more reagents, and a higher amount of dye may be considered as a disadvantage for the method introduced by Ha et al.

Even though there are many reports regarding how to control the size and uniformity of nanoparticles, some of the methods have been successful at producing particles >30 nm, whereas others have focused on the preparation of particles <30 nm. In addition, controversial results regarding the effect of amount of reagents on particle size were reported in the silica literature, although silica chemistry is well understood. Synthesis of particles by the Stöber method usually resulted in a polydispersed size distribution for the size <50 nm. Therefore, a systematic study of controlling the solution chemistry is needed to explore how to control size and uniformity of particles. The aim of our study is systematically to control and tune the hydrodynamic size of fluorescent silica particles by varying the concentrations of the reagents and solvent.

Here we report a systematic method to produce uniform fluorescent particles by modifying the Stöber method. How relative amounts of reagent influence the particle size, monodispersity, and photophysical properties is investigated here in detail. We showed that the amount of ethanol and ammonia precisely tunes the size of silica nanoparticles. Lastly, we evaluated size-dependent cytotoxicity of the fluorescent silica nanoparticles against cancer cell lines.

EXPERIMENTAL SECTION

Tetraethyl orthosilicate (TEOS) and fluorescein isothiocyanate (FITC, isomer I) were purchased from Fluka. 3-Aminopropyl triethoxysilane (APTES, Alfa Aesar), NH_4OH (ammonium hydroxide, 25 wt %, Merck), and ethanol (Riedel) were used as received. Deionized (DI) water was used throughout the study.

In a typical synthesis, APTES (0.385 mmol) and FITC (0.0135 mmol) were dissolved in 1.0 mL of absolute ethanol in the dark and stirred magnetically for ∼18 h at room temperature under a nitrogen atmosphere. The stock solution of the APTES−FITC conjugate was kept in the dark to prevent photobleaching and later used as a fluorescent silane reagent for the production of the fluorescent part of the nanoparticles. For formation of a silica network around the APTES−FITC conjugate, appropriate amounts of ammonia, ethanol, and TEOS given in Table 1 (22 independent batches) were mixed in a 100 mL round-bottomed flask with a magnetic stirring. Reaction times were kept constant for each experiment to prevent adventitious kinetic factors. The solution was allowed to stir for 24 h. Lastly, 245 μL of TEOS was added as the postcoating step for particles and stirred for 24 h more in the same reaction flask. This last step provides a facile means by which to modify the surface of particles via a rich library of silicates. The FITC-conjugated silica particles were washed four times with ethanol to remove unconjugated dyes and other reagents. The purified samples were then dried under nitrogen for physicochemical characterization.

The size and uniformity of the synthesized particles were measured by SEM (scanning electron microscope, Phillips (FEI) XL30- SFEG) and DLS (dynamic light scattering, Zetasizer-3000HSA). Absorption and fluorescence spectra were recorded by Varian Cary 50 UV−visible and Varian Eclipse fluorescence spectrophotometers, respectively. ^{29}Si NMR measurements were carried out on a Bruker Avance 500WB 99 MHz NMR

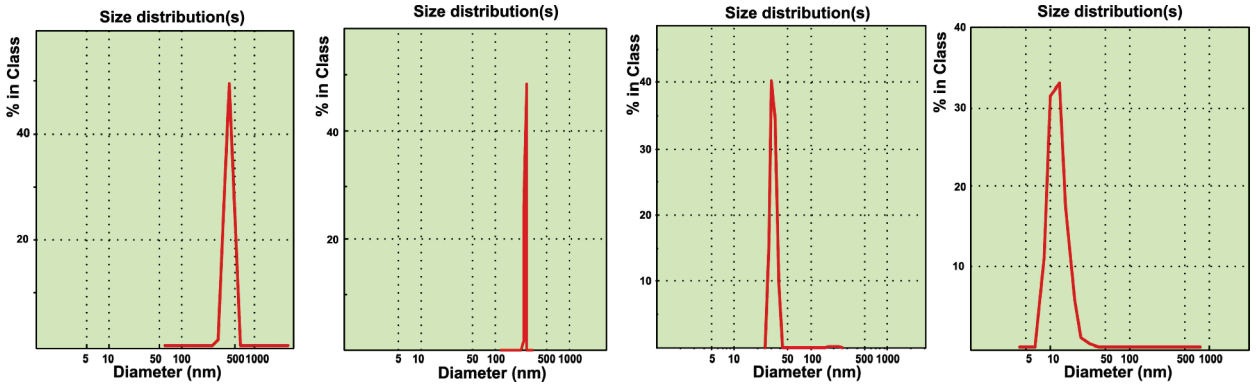

Figure 1. DLS histograms for particles with sizes of 466, 255, 31, and 12 nm (exp. no; 2A, 2B, 2F, 2G), respectively. Amount of ethanol was varied between 60 and 5 mL by keeping the amount of 0.1 mL of APTES-FITC, 1.2 mL of ammonia, and 1.2 mL of TEOS constant.

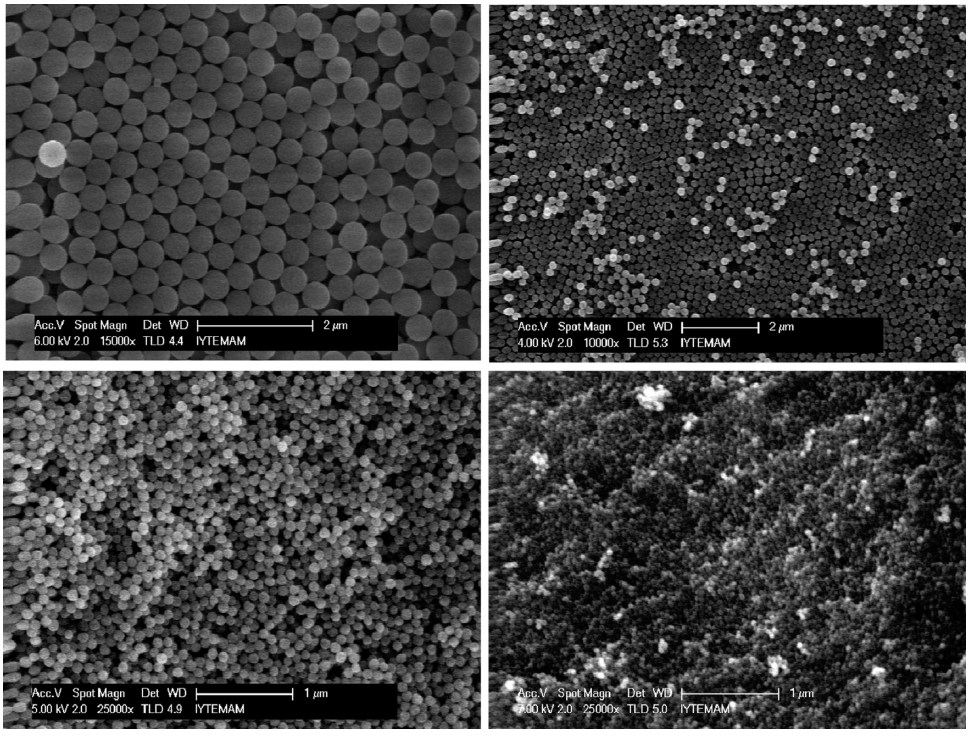

Figure 2. Representative SEM images of FITC-conjugated to silica nanoparticles. Particle sizes are (A) 460, (B) 190, (C) 42, and (D) 30 nm.

spectrometer. ^{13}C NMR experiments were performed with a Bruker 400 MHz spectrometer.

Viability of cell lines of MCF7 and PC3 was evaluated by MTT assay. Particles with the size of 12, 48, and 255 nm were dispersed in PBS with dosages up to 1000 μg/mL. Incubation times were varied up to 72 h.

RESULTS

Silica particles on nanometer scales were prepared by a procedure based on a modified Stöber method, as described in the Experimental Section. To tune and optimize particle size during preparation of each batch, the amount of one of the reagents was systematically adjusted, whereas the amounts of the other reagents were kept constant; in total there were 22 independent batches. Table 1 summarizes the amounts of reagents, experimental conditions, and measurements of the hydrodynamic size of silica particles.

The first series of experiments (the set of exp. no. 1) dealt with the amount of ammonia that was varied in range of 0.3 to 4.8 mL (0.13 to 1.78 M). The hydrodynamic size of particles was determined by DLS measurements, confirming that particle size distributions were monodispersed (standard deviations given in Table 1). Figure 1 shows representative results of hydrodynamic size distributions of particles prepared under a different set of conditions. The size and shape of particles were verified by SEM images, as shown in Figure 2, illustrating that the particles were uniformly spherical.

Following evidence that the particles were monodisperse, the relationship between the size and the initial amount of reagents was analyzed in detail. A plot of particle size versus the volume of ammonia (Figure 3A) indicated two regions around a turning

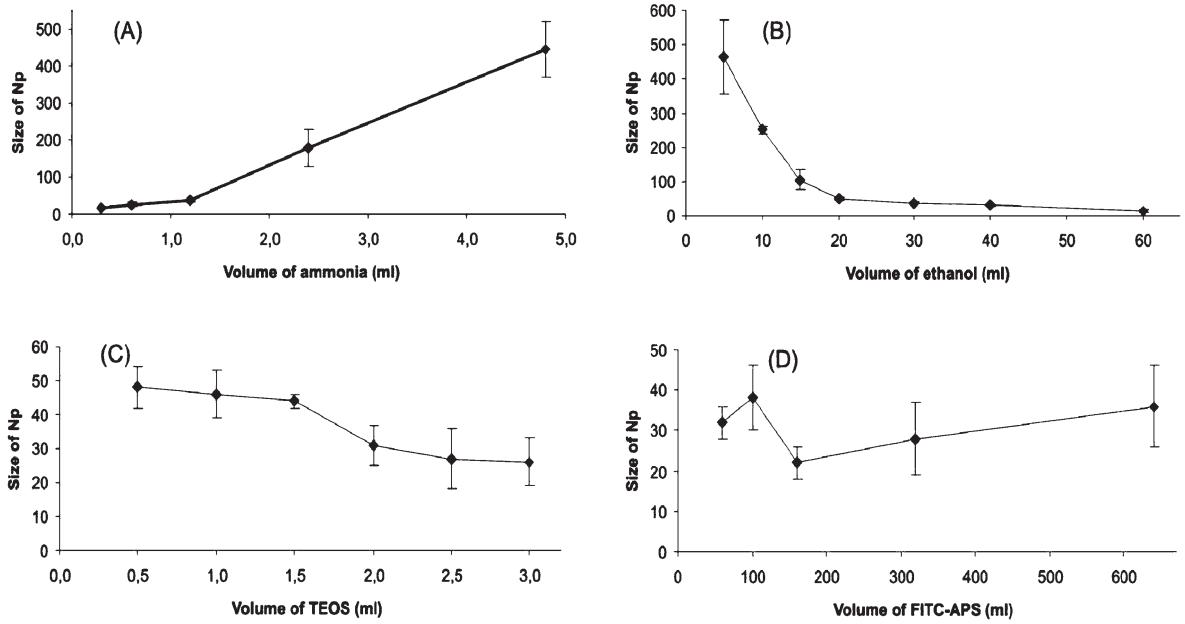

Figure 3. Plots showing dependence of particle size on initial amount of reagents: (A) ammonia, (B) ethanol, (C) TEOS, and (D) APTES-FITC. Size of particles exponentially decreases with increasing amount of ethanol and increases with ammonia.

point of 1.2 mL (0.49 M). The size of particles in both regions was linearly proportional to the amount of ammonia. For experiments where >1.2 mL ammonia was used in the reaction, the particle becomes larger as a function of the initial volume of ammonia increasing. This result suggests that silica particles in a desired size can be produced by simply adjusting the initial amount of ammonia within the conditions provided here.

All reactions including the synthesis of the fluorescent conjugate and formation of the silica network were performed in the presence of ethanol. Therefore, ethanol is the solvent of the reaction medium in this work. The amount of ethanol was adjusted from 60.0 to 5.0 mL (Table 1, the set of exp. no. 2). Ethanol produced during the hydrolysis of TEOS was not taken into account because a constant amount of TEOS was used in the set of exp. no. 2. The effect of the amount of ethanol on the size of the particles is presented in Figure 3B. The adjustment of the volume of ethanol yields highly uniform nanoparticles in the size range from 12 to 465 nm. As shown in Figure 3B, there is an exponential dependence of the particle size to the initial volume of ethanol. The exponential dependence indicates that the initial amount of ethanol is the major factor regulating the particle size.

After determining how amounts of ammonia and ethanol tune the size of particles, we studied the effect of the amount of TEOS on the size. The amount of TEOS was increased from 0.5 to 3.0 mL (Table 1, the set of exp. no. 3). Figure 3C shows that amounts of TEOS up to 1.5 mL were not effective within the experimental error on the particle size (~45 nm); however, when the amount of TEOS was >1.5 mL, the particle size was meaningfully reduced to 25 nm. The change in particle size was not proportional to the amount of TEOS in the reaction flask, although the amount of TEOS increased by a factor of 6. Therefore, the variation in the amount of TEOS does not greatly affect the particle size in the concentration range used in this study, as compared with the profound effects of the amount of ammonia and ethanol.

We next investigated the amount of APTES-FITC conjugate on particle size (Table 1, the set of exp. no. 4). DLS results showed that particle size varied with increasing amounts of APTES-FITC (Table 1). There was a fluctuation in size when a lower amount of APTES-FITC conjugate (<0.1 mL) was employed. The particle size was increased in a linear fashion as the amount of the conjugate was increased, as shown Figure 3D. The effect of the amount of conjugate on particle size is determined to be not substantial.

Under these experimental conditions, the results point out that the amount of ammonia and ethanol are very effective to tune the hydrodynamic size of particles. The two other reagents, TEOS and APTES-FITC conjugate, played a limited role in the size and monodispersity of particles under the experimental conditions presented here.

^{13}C and ^{29}Si CP-MAS NMR spectroscopy are powerful methods for characterizing the chemical structure of substances that can be prepared from (organo)-alkoxysilanes.[31,53] Using these methods, it is also possible to obtain information about the surface characteristics of silica particles such as the type and amount of coverage and the number of the bonds that have been formed in the coating reactions. ^{29}Si CP-MAS NMR spectra revealed well-defined broad lines, as expected, at −111.4 (Q^4), − 101.5 (Q^3), and −92.7 (Q^2) ppm (Figure 4A). It is easy to distinguish among the Q^4, Q^3, and Q^2 silicons because their chemical shifts are all separated by ~10 ppm. The existence of an Si−C bond causes a shift at ~45 ppm; again, there is a separation of ~10 ppm among the T^3, T^2, and T^1 silicons.[31] However, such formations were not observed, except for a tiny peak at −67.4 ppm that can be ascribed to T^3 silicons. ^{13}C CP-MAS NMR measurements were used to characterize qualitatively the fate of the ethoxy and aminopropyl groups of the (organo)-alkoxysilanes on the particle surface (Figure 4B). Two major ^{13}C−NMR signals were observed at 17.7 and 59.1 ppm that were attributed to the equivalent carbons of the $-CH_3$ and $-O-CH_2-$ of TEOS, respectively. However, the formation of small peaks at 10.0 ($Si-CH_2$), 23.5 ($-CH_2-CH_2-CH_2-$), and 43.1 ppm ($-CH_2-NH_2$) can be ascribed to APTES (Figure 4B). These spectra are considered to

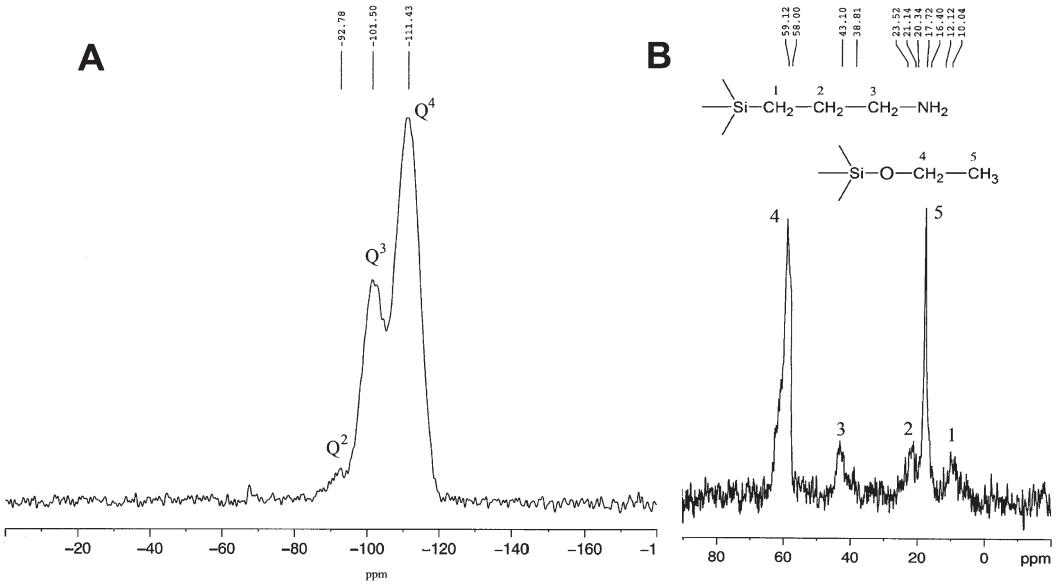

Figure 4. (A) ^{29}Si CP-MAS NMR and (B) ^{13}C CP-MAS NMR spectra of particles.

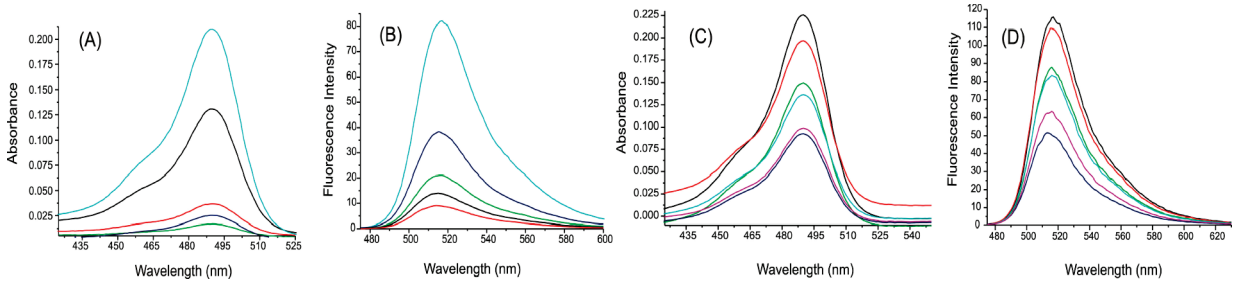

Figure 5. Absorption (A,C) and fluorescence spectra (B,D) of FITC released by disintegrating 5 mg/mL of silica particles in 1 M NaOH. Excitation wavelength is 490 nm. The particles prepared by the set of experiments exp. no. 1. and exp. no. 2 were used. Disintegrated FITC molecules were separated by centifugation.

be proof of the existence of $-NH_2$ groups in the particle structure, although an additional amount of TEOS was used at the post coating step. Overall, NMR measurements along with microscopic and spectroscopic measurements identified the formation of siloxane bonds and silica particle formation.

It is important to control the number of FITC molecules conjugated to silica particles. To determine the amount of conjugated FITC, we intentionally disintegrated the silica particles in a 1 M aqueous solution of NaOH. Figure 5 shows the absorption and fluorescence spectra of FITC released as a result of the degradation of silica particles prepared in the set of exp. no. 1. Figure 5A shows an increase in absorbance as the particle size was increased. The released number of FITC molecules was determined by absorbance measurements of the supernatant obtained as a result of the disintegration of silica particles. The amount of FITC released in the solution was determined to be from 0.02 μM for the smallest particle to 1.40 μM for the largest one. This indicates that the number of FITC molecules disintegrated from the particles increased as the particles became larger, with supporting evidence being that the larger particles contained a higher number of FITC molecules. Similarly, Figure 5B demonstrates that the intensity of fluorescence was amplified for larger particles. These results verify that there is a linear relationship between the number of FITC molecules conjugated to particles and particle size. The results lead us to conclude that the density of the FITC molecules per particle is equivalent. The same results (Figure 5C,D) were observed when the size of the particles varied as a function of the amount of ethanol (the set of exp. no. 2); there is an exponential trend. Figure 6, a 3D plot, reveals the relationships among size, absorbance, and fluorescence intensity.

To confirm whether the silica network protects dye molecules, we treated the particles with environmental factors such as solvents, pH, and quenchers. The fluorescence spectra of FITC molecules both dissolved in and conjugated to the silica particles dispersed in dimethyl formamide, ethanol, and water are presented in Figure 7. The shape of the fluorescence spectra of FITC dissolved in the solvents changed, and the peak position shifted to red because of the solvatochromatic effect (increased orientational polarizability) as the solvent molecules interact freely with FITC molecules. However, the spectra of FITC conjugated to the particles (Figure 7B) showed no variation with the solvents. Apparently, the solvent molecules do not reach the FITC molecules conjugated to the particle; an effective protection layer against solvents has been provided by the silica network for FITC molecules.

Fluorescence quenching is a process causing a reduction in the fluorescence intensity of a fluorophore if a quencher interacts with the fluorophore. Accordingly, quenching studies can be

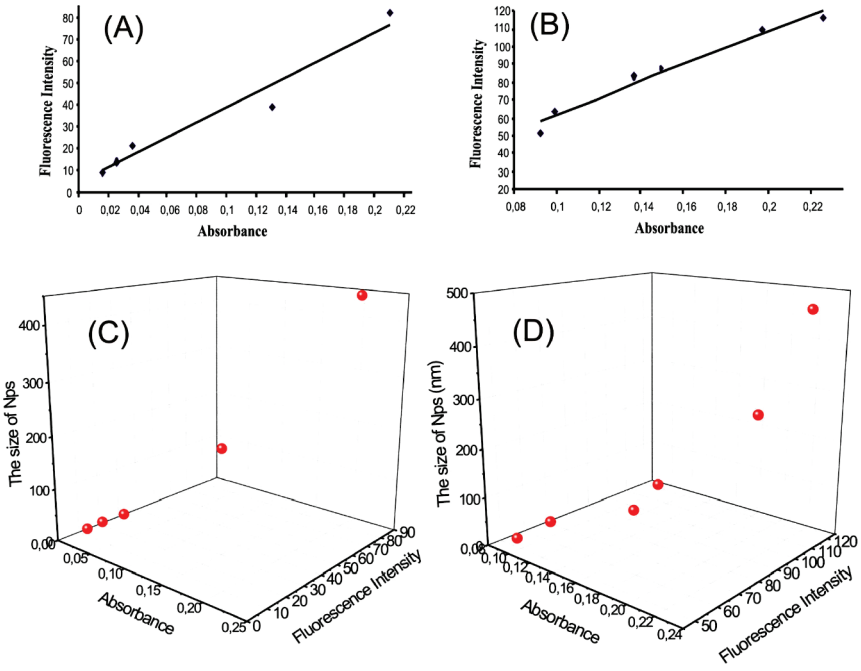

Figure 6. Graphs (A,B) were plotted for fluorescence intensity versus absorbance for the set of experiment 1 (1A to 1E in the Table 1) and the set of experiment 2 (2A to 2F). 3D plots (C and D) of particle size versus fluorescence intensity and absorbance are shown. The correlation coefficient R^2 (for the exp. set of 1) = 0.9522, R^2 (for the exp. set of 2) = 0.9665. The graphs on the left are related to effect of amount of ammonia; the plots on the right show the effect of amount of ethanol.

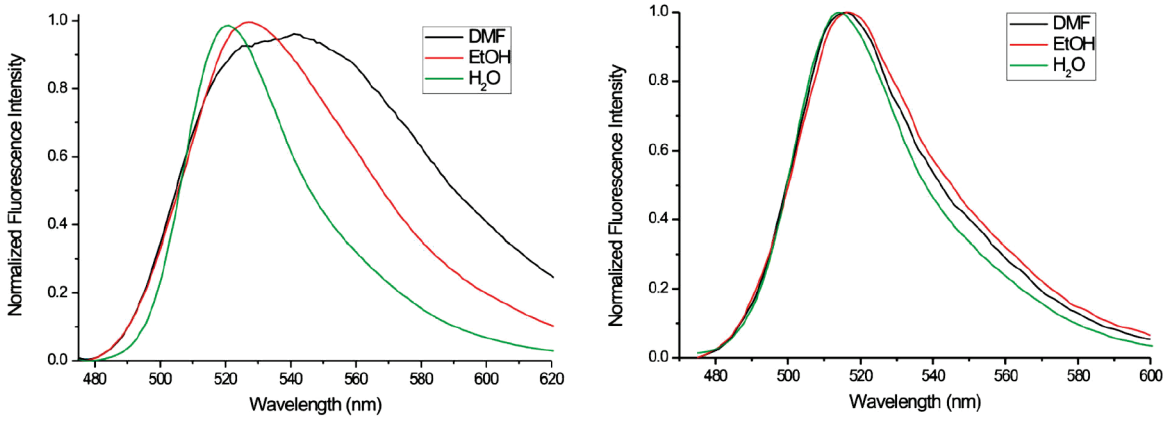

Figure 7. Solvent effect: fluorescence spectra of free FITC (left) dissolved in water and FITC conjugated to particles (right) dispersed in different solvents, dimethyl formamide (DMF), ethanol (EtOH), and water (H_2O).

used to reveal the interaction of a quencher with dye molecules conjugated to silica. We performed fluorescence quenching studies by using $CuCl_2$ and KI as quenchers to assess the protection ability of the silica network for dye molecules against the quenchers. The fluorescence spectra of FITC conjugated-silica particles with the size of 30 and 180 nm dispersed in aqueous solutions were recorded. The Stern−Volmer plots were obtained for the assessment of quenching. For comparison, the aqueous solutions of FITC were also prepared, and its fluorescence was monitored by increasing the amount of the quenchers. Figure 8 depicts the Stern−Volmer plots, showing that quenching of FITC in aqueous solutions by Cu^{2+} and I^- ions is strong, but the FITC conjugated to the particles is weakly affected by the quenchers depending on its type and amount. When the $[Cu^{2+}]$ is >0.1 M, a precipitation was observed, limiting the quenching study for higher concentrations. The negatively charged quencher I^- interacts with FITC conjugated to particles, and the fluorescence intensity was quenched to a certain extent, quantified by the Stern−Volmer coefficient, $K_{SV(FITCconjugated)}$, which is calculated to 3.5. The quenching of FITC in aqueous solution was substantial and was quantified by the coefficient $K_{SV(FITC\text{-}free)}$ to be equal to 15.1. By comparing the SV coefficients, we see that FITC molecules easily interact with quenchers in aqueous solution. The silica network provides a certain level of protection for FITC-conjugated to the particles. It indicates that the quencher ions are able to penetrate into the silica network and interact with some of the FITC molecules presumably close to the surface of the particles. Diffusion ability of the quenchers to the conjugated FITC indicates that

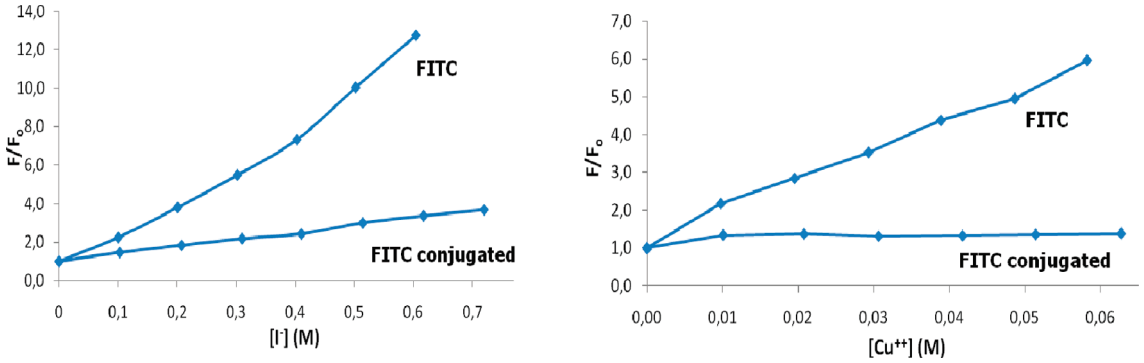

Figure 8. Quenching effect: Stern−Volmer plots of free FITC and FITC-conjugated silica particles in the presence of quenchers (A) I^- and (B) Cu^{2+} ions.

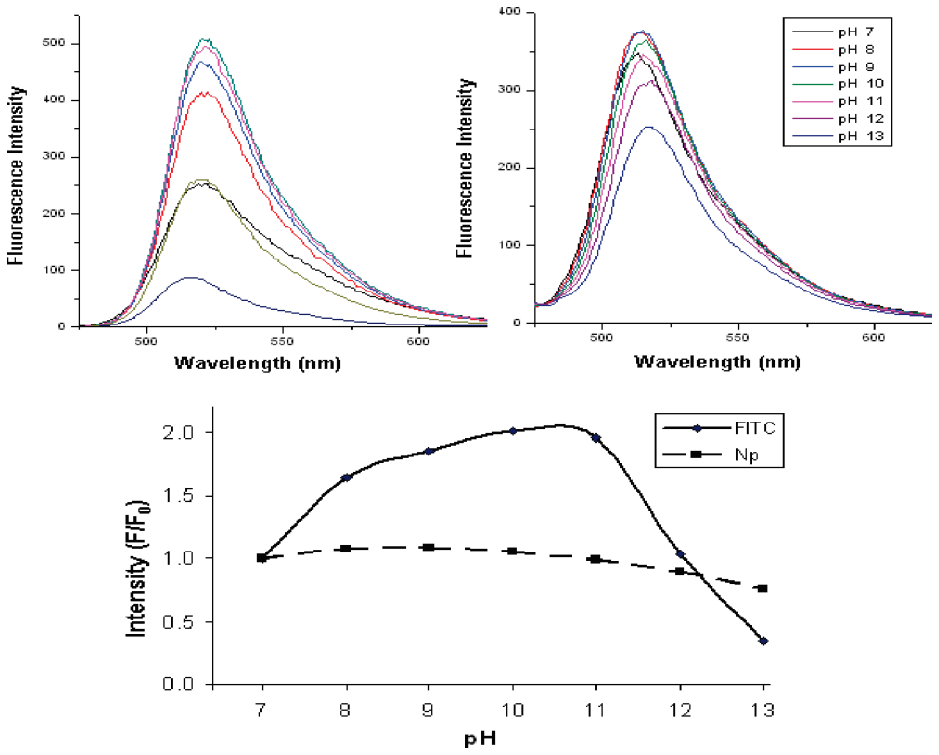

Figure 9. pH dependence of fluorescence spectra for free FITC (on the left) and particles (on the right). The pH of the solution was varied from 7 to 13. The pH dependence of fluorescence intensity is shown by taking the intensity at pH 7 as reference. Solutions with higher pH values cause a reduction in the fluorescence intensity of FITC.

the silica particles may possess an open structure or surfaces that allow ions to diffuse the silica network.

It is well known that the pH of the environment through protonation of FITC modulates fluorescence intensity; therefore, the fluorescence of FITC is sensitive to solution pH of its environment. Investigating the influence of pH on FITC conjugated to particles could further demonstrate the protective nature of the silica matrix. The pH of the aqueous solution was adjusted from 6 to 13. Figure 9 represents how the pH of the solution makes an impact on the fluorescence spectra of FITC in solution or conjugated to silica particles. Reduction in the fluorescence intensity was observed for FITC when dissolved in aqueous solution, but the intensity of the FITC-conjugated to particles remained almost unchanged. There was a 30% decrease in intensity for pH higher than 11 that indicates the disintegration of the particles. The spectral shape and position also did not change with pH. These findings confirmed the protection provided by the silica matrix to FITC against changes in pH of the environment.

Photostability performance of the particles was checked by photobleaching of FITC emission. The test was applied to particles containing different amounts of dye molecules (Table 1, exp. no. 4). Variation in the fluorescence intensity of the particles with time was monitored for up to 100 min under continuous illumination. It was observed that the fluorescence intensity reduced rapidly within 5 min and remained unchanged after 20 min, as seen in Figure 10. The fluorescence intensity of particles containing higher amounts of APTES-FITC conjugate was determined to be decreased by 3 and 13% at 5 and 100 min, respectively. The intensity was decreased by 5% at 5 min and by 21% at 100 min for the particles with a lesser

amount of the conjugate. The rate of photobleaching was greater for the particles containing a lower number of dye molecules. These measurements illustrated that particles encapsulating a higher number of FITC molecules are much brighter for a prolonged period of time. This photobleaching might be due to interactions between FITC molecules in close proximity conjugated to particles.

Assessment of cell viability is important for the biological and medical applications of silica particles. Figure 11 shows the results of size-dependent cell viability determined by the MTT assay for MCF7 and PC3 cells. Cells were incubated with the particles (size of 12 to 255 nm) at dosages up to 1000.0 μg/mL. Incubation times up to 72 h were employed. Under these experimental conditions, cell viability of MCF7 and PC3 cells with respect to particle size, dosage, and incubation time remained unchanged. The results point out no size-dependent cytotoxicity. Silica particles do not stimulate cell death on MCF7 and PC3 cell lines.

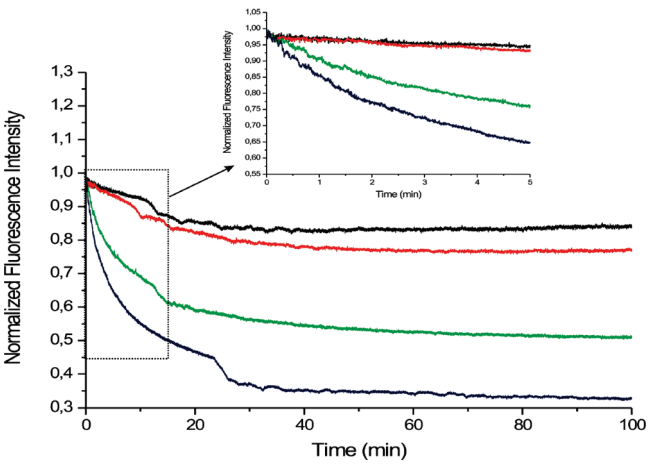

Figure 10. Assessment of photostability of silica particles by continuous illumination by a pulsed Xe lamp. Amount of FITC encapsulated in particles varied but the size of particles is constant around 30 nm. Black, exp. no. 4E; red, exp. no. 4D; blue, exp. no. 4C; green, exp. no. 4B.

DISCUSSION

The discussion section is mainly devoted to particle formation. Hydrolysis and condensation of silicates leads to the formation of silica particles. Concurrently, solution chemistry is important for the formation of these particles. In this work, on the basis of a modified Stöber method, the initial amounts of reagents were systematically varied to better elucidate the role of each reagent on the hydrodynamic size of fluorescent silica nanoparticles.

The formation of silanols $[(EtO)_3SiOH$ and $(EtO)_2Si(OH)_2]$ as key intermediates during TEOS polymerization is well known. Condensation of silanol, $\equiv$Si$-$O$-$H, as an intermediate via an SN_2 mechanism, yields the siloxane bonds, $\equiv$Si$-$O$-$Si$\equiv$. Under base-catalyzed conditions there is an equilibrium between the hydroxide and ethoxide nucleophiles because of the similar pK_a values of their conjugate acids. Nucleophilic attack of the ethoxide ion to a silicon center of TEOS will not yield the formation of any product (Scheme 1). Nucleophilic attack of a hydroxide ion to the silicon center will produce a silanol structure that is more acidic than ethanol. A Bronsted acid$-$base reaction will form a nucleophilic silyloxide, which will react further with a second TEOS molecule to form a $\equiv$Si$-$O$-$Si$\equiv$ bond (Scheme 1). An increase in the concentration of ethanol may

Scheme 1. Formation of Silanol and Siloxane Bonds

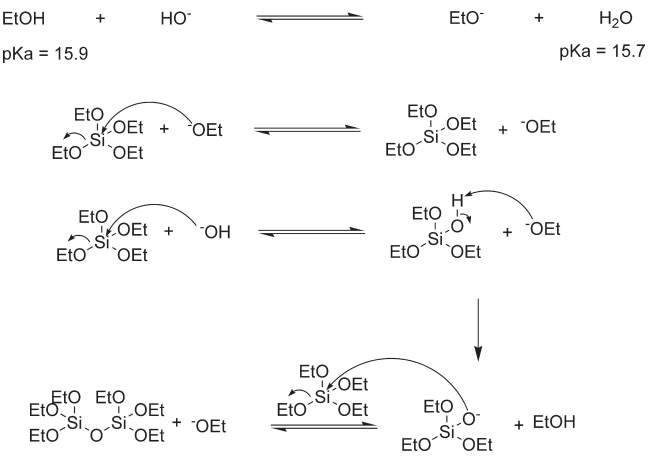

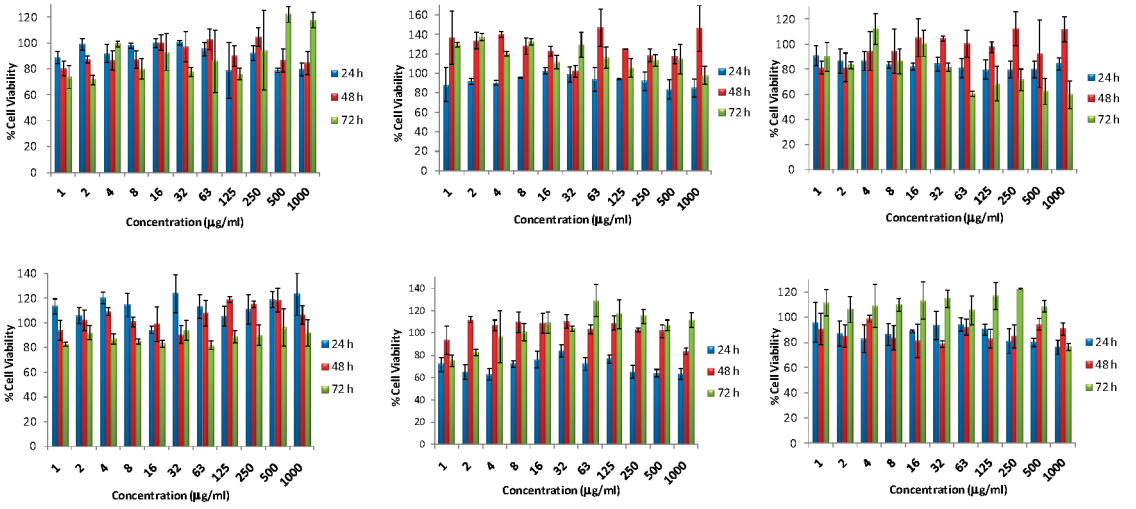

Figure 11. Cell viability assayed by MTT for the cell lines MCF 7 and PC3. Variables are particles with different sizes (12, 48, 251 nm), incubation times (24, 48, 72 h), and dosages (1$-$1000 μg/mL).

dx.doi.org/10.1021/jp204323d |J. Phys. Chem. C 2011, 115, 16322–16332

shift the equilibrium to the right, thus increasing the concentration of ethoxide ions and decreasing the concentration of hydroxide ions. Such control over the hydroxide ion concentration plays a key role in the nucleation and growth and therefore the size of the silica nanoparticles.

As explained in Scheme 1 the concentration of ethanol in the reaction medium is critical to the formation of siloxane bonds. We found that the size of particles exponentially decreased with increasing initial amount of ethanol (11−16 M in the presence of 0.49 M ammonia), as shown in Figure 3B. Higher amounts of hydroxide ions are available when lower volumes of ethanol are used, thus yielding more interactions between the initial nucleate and hydrolyzed monomer. The number of interactions decreases with the increasing amount of ethanol. Ethanol and methanol as solvent were used in some studies.[30,56,57] Smaller particles were formed in methanol as compared with ethanol. However, in the literature, neither ethanol nor methanol has been progressively varied to comprehend the effect of solvent on the size of silica particles. In one particular study, Rao et al. showed that ethanol in the range of 4−10 M (in three different batches) yielded an increase in the size of particles in the presence of 14 M ammonia. The increase in particle size may be attributed to the presence of a very high concentration of ammonia, producing an excess amount of hydroxide ions in the reaction medium. There is a consensus in the literature that a progressive increase in the amount of water yields the formation of larger silica nanoparticles. We verified the effect of increased amounts of water on the size of particles.

The amount of ammonia strongly controls the particle size, and our results agree very well with the literature. Ammonia served as a reactant and a catalyst for the hydrolysis of TEOS. One of the reactant OH^- ions provided by ammonia is important for the formation of particles. The literature shows that the concentration of the basic catalyst is responsible for tuning particle size.[39,44,47−51,54−64] In our study, we systematically varied the amount of ammonia from 0.13 to 1.78 M and showed that the size of the particles increased as the amount of ammonia was increased. The reports regarding the effects of ammonia on the size of particle are controversial. Rao et al. observed that the size of particle decreased with increasing the ammonia concentration (2.80−28.0 M) in the presence of 1.0−8.0 M ethanol and 3.0−14.0 M water.[62] Bagwe et al. showed that the increase in the amount of ammonia (0.16 to 0.64 M) yielded larger particles.[50] In addition to these, Ha et al. reported that the greater the amount of ammonia, the larger the particle size,[51] but they concurrently increased the amount of water (2.0−7.8 M) and the reaction time. Furthermore, Wiesner and Ow showed that larger particles (100−500 nm) were obtained in the presence of higher amounts of ammonia (3.4−6.1 M) and water (10.8−16.8 M), whereas particles <100 nm were prepared with a decreased amount of ammonia (0.2 to 0.0085 M).[63] Tan et al. controlled the size of particles and demonstrated that the particle size was decreased from 70 to 25 nm when the amount of ammonia was reduced to three-fold of its initial value.[10,11] These reports clearly point out that the solution chemistry is detrimental to tune the size of particle. A systematic investigation to generate a set of data regarding the effect of the amounts of reagents on the size of particles is essential. However, each report used a different set of experimental conditions, and the concentration of reagents was not systematically varied. Our study clears the inconsistency among the results reported in the literature.

The influence of the amount of TEOS on particle size is limited in our study (16 M ethanol, 0.49 M ammonia). Many studies in the literature again are controversial. Tunability on the particle size as a function of the increased concentration of TEOS has been studied.[49−51,60−62] Bagwe et al. reported that there was no change in particle size when they increased the concentration of TEOS from 0.025 to 0.1 mM.[50] Rao et al. found that as the concentration of TEOS was increased from 0.012 to 0.12 M, an increase in particle size from 60 to 417 nm was obtained in the presence of 8 M ethanol, 3 M water, and 14 M ammonia.[62] Yokoi et al. reported that TEOS increased the particle size 3-fold (∼12−36 nm), although the amount of TEOS was increased 12-fold (from 1 to 12 M).[49] It is well known that four moles of ethanol are produced for each mol of TEOS during the hydrolysis and condensation reactions. Thus, the initial amount of TEOS contributes to the total amount of ethanol in the reaction medium. We already stated that the amount of ethanol is the most important parameter to control the size of particles. An increase in the amount of hydrolyzed ethanol may cause a reduction in the size of the particle as the concentration of TEOS increased. This is exactly what we observed.

As expected, the amount of APTES−FITC conjugates did not have an impact on particle size. Imhof et al. investigated the effect of the APTES−FITC conjugate amount by varying the conjugate concentration between 10 and 640 μL.[39] In their experiments, the conjugate was steadily increased; as a result, particle size increased slightly from 200 to 250 nm. They obtained their largest particles when the amount of the FITC conjugate was increased from 320 to 640 μL in different volumes of ethanol. Our work validates the fact that the particle size is not greatly affected by amount of the FITC-conjugate, but silica particles are much smaller under the experimental conditions presented when the fluorescent conjugate is not added during the synthesis. The separate set of experiments in the absence of the fluorescent conjugate is summarized in the Supporting Information.

Many biological applications rely on fluorescence properties such as intensity and emission wavelength, and thus it is desirable to have fluorescent particles with spectral features that remain unaffected by the environmental factors. Solvent, pH, and ions in solutions or cellular environment may change spectral properties of fluorescent particles if the fluorophore that is conjugated to silica is accessible to the environment. We show that the silica network keeps the spectral properties of FITC unaffected against the pH of the solution and the solvent. This is imperative for biological applications such as tracking the motions of proteins and the locations of drug carriers. Such applications depend on stable fluorescence intensity because the motions and locations of proteins and DNA may be probed by a fluorescent molecule or a single fluorescent particle. Fluorescent silica particles may contain many fluorophores; therefore, the particles may emit for a longer period of time, allowing an extended period of observation. Only a limited number of fluorescent probes may present such stability. Many probes report fluctuations and variations of their environment.

Biocompatible, biodegradable, and nontoxic materials are required for biological and medical applications. Silica is shown to possess these features, and, as a result, it is a biomaterial of choice. To this end, we demonstrated that the fluorescent silica particles produced in this work are not toxic against cancer cells MCF7 and PC3. Many studies agree that silica is not toxic at all and safe for use in biological applications. For medical application, it is crucial that the hydrodynamic diameter of silica nanoparticles must be <7.0 nm to be cleared from body.[45] This indicates that the hydrodynamic size of silica must be reduced for clinical applications such as the safe delivery of drugs to tissues

and organs. This fact requires more systematic work to figure out how to reduce the hydrodynamic size of silica particles, albeit one study already has been reported by the Wiesner group.[45] It is reported that silica particles are approved by the FDA for the first clinical trials. Surface potential, basicity, and acidity of silica surfaces are important factors to elucidate the fate of the silica particle for biological and medical applications. We will direct our attention to these areas and extend our work to determine the locations and motions of fluorescent silica particles in normal and cancerous cell lines as a function of surface chemistry and surface potentials.

CONCLUSIONS

We present a method to synthesize systematically monodispersed FITC conjugated silica particles by using a modified Stöber method. The hydrodynamic size of fluorescent particles was tuned in the range from 12 to 465 nm. We demonstrated that the systematic control of hydrodynamic size of particles can be achieved by regulating the solution chemistry. We showed that the size strongly depends on the amount of ethanol and ammonia. Higher amount of ethanol regulated the concentration of hydroxide ion, leading to controlled growth of the silica particles and resulting in precise tuning of the hydrodynamic size. Moreover, we showed that the amount of dye conjugated to the particles can be controlled by the size of the particles. The concentration of FITC molecules conjugated to particles was varied between 0.02 and 1.40 μM. The silica network protects FITC molecules against pH and solvent and partially against ionic quenchers. The penetration ability of ionic quenchers may be interpreted that silica particles may have open structure on the subnanometer scale on the surface of the particles because solvent molecules do not reach conjugated FITC molecules to induce solvent effects. We propose that fluorescent silica nanoparticles may possess an open structure on the surface of the particles and may not have a fluorescent core/silica shell structure, as assumed in the literature. Furthermore, the silica particles are not cytotoxic up to 1.0 mg/mL and up to 72 h of incubation period, respectively. The particles may be ready for biological applications, but they are not ready for medical applications without evidence of their clearance from the body. Moreover, other biological functions such as inflammation and genotoxicity must be studied because the biological response of cells is not limited to cytotoxicity.

ASSOCIATED CONTENT

Supporting Information. Effects of reagents on particle size (no APTS-conjugated FITC used). This material is available free of charge via the Internet at http://pubs.acs.org.

AUTHOR INFORMATION

Corresponding Author

*E-mail: serdarozcelik@iyte.edu.tr. Tel: 90 232 750 7557.

Present Addresses

[†]Advanced Technologies Research & Application Center, Mersin University, TR-33343 Yenisehir, Mersin, Turkey.

ACKNOWLEDGMENT

This work was partially supported by TUBITAK (project number 108T446) and DPT (the State Planning Organization of Turkey). We thank Muhsin Ciftcioglu and Ali Cagir for fruitful discussions and Ritchie Eanes for proofreading of the manuscript. We acknowledge that part of the studies was carried out at IYTE-MRC and IYTE-Biyomer.

REFERENCES

(1) Rosi, N. L.; Mirkin, C. A. Nanostructures in biodiagnostics. *Chem. Rev.* **2005**, *105*, 1547.

(2) Zhao, X. J.; Bagwe, R. P.; Tan, W. H. Development of organic-dye-doped silica nanoparticles in a reverse microemulsion. *Adv. Mater.* **2004**, *16*, 173.

(3) Bringley, J. F.; Penner, T. L.; Wang, R.; Harder, J. F.; Harrison, W. J.; Buonemani, L. Silica nanoparticles encapsulating near-infrared emissive cyanine dyes. *J. Colloid Interface Sci.* **2008**, *320*, 132.

(4) Santra, S.; Zhang, P.; Wang, K. M.; Tapec, R.; Tan, W. H. Conjugation of biomolecules with luminophore-doped silica nanoparticles for photostable biomarkers. *Anal. Chem.* **2001**, *73*, 4988.

(5) Santra, S.; Wang, K. M.; Tapec, R.; Tan, W. H. Development of novel dye-doped silica nanoparticles for biomarker application. *J. Biomed. Opt.* **2001**, *6*, 160.

(6) Santra, S.; Liesenfeld, B.; Bertolinoa, C.; Dutta, D.; Caoc, Z. H.; Tan, W. H.; Moudgil, B. M.; Mericle, R. A. Fluorescence lifetime measurements to determine the core−shell nanostructure of FITC-doped silica nanoparticles: an optical approach to evaluate nanoparticle photostability . *J. Lumin.* **2006**, *117*, 75.

(7) Santra, S.; Yang, H.; Dutta, D.; Stanley, J. T.; Holloway, P. H.; Tan, W. H.; Moudgilb, B. M.; Mericle, R. A. TAT conjugated, FITC doped silica nanoparticles for bioimaging applications. *Chem. Commun.* **2004**, *24*, 2810.

(8) Lian, W.; Litherland, S. A.; Badrane, H.; Tan, W. H.; Wu, D. H.; Baker, H. V.; Gulig, P. A.; Lime, D. V.; Jin, S. G. Ultrasensitive detection of biomolecules with fluorescent dye-doped nanoparticles. *Anal. Biochem.* **2004**, *334*, 135.

(9) Yang, W.; Zhang, C. G.; Qu, H. Y.; Yang, H. H.; Xu, J. G. Novel fluorescent silica nanoparticle probe for ultrasensitive immunoassays. *Anal. Chim. Acta* **2004**, *503*, 163.

(10) Wang, L.; Yang, C.; Tan, W. Dual-luminophore-doped silica nanoparticles for multiplexed signaling. *Nano Lett.* **2005**, *5*, 37.

(11) Wang, L.; Tan, W. Multicolor FRET silica nanoparticles by single wavelength excitation. *Nano Lett.* **2006**, *6*, 84.

(12) Bagwe, P. R.; Hillard, L. R.; Tan, W. Surface modification of silica nanoparticles to reduce aggregation and nonspecific binding. *Langmuir* **2006**, *22*, 4357.

(13) Gao, F.; Luo, F. B.; Yin, J.; Wang, L. Preparation of aminated core-shell fluorescent nanoparticles and their application to the synchronous fluorescence determination of gamma-globulin. *Luminescence* **2008**, *23*, 392.

(14) Hun, X.; Zhang, Z. J. Functionalized fluorescent core-shell nanoparticles used as a fluorescent labels in fluoroimmunoassay for IL-6. *Biosens. Bioelectron.* **2007**, *22*, 2743.

(15) Shi, H.; He, X.; Wang, K.; Yuan, Y.; Deng, K.; Chen, J.; Tan, W. Rhodamine B isothiocyanate doped silica-coated fluorescent nanoparticles (RBITC-DSFParticles)-based bioprobes conjugated to Annexin V for apoptosis detection and imaging. *Nanomed.: Nanobiotechnol., Biol., Med.* **2007**, *3*, 266.

(16) Roy, I.; Ohulchanskyy, T. Y.; Bharali, D. J.; Pudavar, H. E.; Mistretta, R. A.; Kaur, N.; Prassad, P. N. Optical tracking of organically modified silica nanoparticles as DNA carriers: a nonviral, nanomedicine approach for gene delivery. *Proc. Natl. Acad. Sci. U.S.A.* **2005**, *102*, 279.

(17) Fuller, E. J.; Zugates, G. T.; Ferreira, L. S.; Ow, H. S.; Nguyen, N. N.; Wiesner, U. B.; Langer, R. S. Intracellular delivery of core-shell fluorescent silica nanoparticles. *Biomaterials* **2008**, *29*, 1526.

(18) Qhobosheane, M.; Santra, S.; Zhang, P.; Tan, W. H. Biochemically functionalized silica nanoparticles. *Analyst* **2001**, *126*, 1274.

(19) Yamauchi, H.; Ishikawa, T.; Kondo, S. Surface characterization of ultramicro spherical-particles of siliva prepared by w/o microemulsion method. *J. Colloids Surf.* **1989**, *37*, 71.

(20) Osseoasare, K.; Arriagada, F. J. Preparation of SiO_2 nanoparticles in a nonionic reserve micellar system. *J. Colloids Surf.* **1990**, *50*, 321.
(21) Lindberg, R.; Sjöblom, J.; Sundholm, G. Preparation of silica particles utilizing the sol-gel and the emulsion-gel processes. *Colloids Surf., A* **1995**, *99*, 79.
(22) Arriagada, F. J.; Osseoasare, K. Synthesis of nanosize silica in aerosol OT reverse microemulsions. *J. Colloid Interface Sci.* **1995**, *170*, 8.
(23) Arriagada, F. J.; Osseoasare, K. Silica nanoparticles produced in aerosol OT reverse microemulsions-effect of benzyl alcohol on particle-size and polydispersity. *J. Dispersion Sci. Technol.* **1994**, *15*, 59.
(24) Arriagada, F. J.; Osseoasare, K. Phase and dispersion stability effects in the synthesis of silica nanoparticles in a nonionic reverse microemulsion. *Colloids Surf.* **1992**, *69*, 105.
(25) Arriagada, F. J.; Osseo-Asare, K. Synthesis of nanosize silica in a nonionic water-in-oil microemulsion: Effects of the water/surfactant molar ratio and ammonia concentration. *J. Colloid Interface Sci.* **1999**, *211*, 210.
(26) Stöber, W.; Fink, A.; Bohn, E. Controlled growth of monodisperse silica spheres in the micron size range. *J. Colloid Interface Sci.* **1968**, *26*, 62.
(27) Burns, A.; Ow, H.; Wiesner, U. Fluorescent core-shell silica nanoparticles: towards "Lab on a Particle" architectures for nanobiotechnology. *Chem. Soc. Rev.* **2006**, *35*, 1028.
(28) Sharma, P.; Brown, S.; Walter, G.; Santra, S.; Moudgil, B. Nanoparticles for bioimaging. *Adv. in Colloid Interfac.* **2006**, *123*, 471.
(29) Van Blaaderen, A.; Imhof, A.; Hage, W.; Vrij, A. Three-dimensional imaging of submicrometer colloidal particles in concentrated suspensions using confocal scanning laser microscopy. *Langmuir* **1992**, *8*, 1514.
(30) Van Blaaderen, A.; Vrij, A. Synthesis and characterization of colloidal dispersions of fluorescent, monodisperse silica spheres. *Langmuir* **1992**, *8*, 2921.
(31) Van Blaaderen, A.; Vrij, A. Synthesis and characterization of monodisperse colloidal organo-silica spheres. *J. Colloid Interface Sci.* **1993**, *156*, 1.
(32) Van Blaaderen, A.; Peetermans, J.; Maret, G.; Dhont, J. K. G. Long-time self-diffusion of spherical colloidal particles measured with fluorescence recovery after photobleaching. *J. Chem. Phys.* **1992**, *96*, 4591.
(33) Nyffenegger, R.; Quellet, C.; Ricka, J. Synthesis of fluorescent, monodisperse, colloidal silica particles. *J. Colloid Interface Sci.* **1993**, *159*, 150.
(34) Burns, A.; Ow, H.; Wiesner, U. Fluorescent core-shell silica nanoparticles: towards "Lab on a Particle" architectures for nanobiotechnology. *Chem. Soc. Rev.* **2006**, *35*, 1028.
(35) Tapec, R.; Zhao, X. J. J.; Tan, W. H. Development of organic dye-doped silica nanoparticles for bioanalysis and biosensors. *J. Nanosci. Nanotechnol.* **2002**, *2*, 405.
(36) Wang, L.; Wang, K. M.; Santra, S.; Zhao, X. J.; Hilliard, L. R.; Smith, J. E.; Wu, J. R.; Tan, W. H. Watching silica nanoparticles glow in the biological world. *Anal. Chem.* **2006**, *78*, 646.
(37) Lettinga, M. P.; van Zandvoort, M. A. M. J.; van Kats, C. M.; Philipse, A. P. Phosphorescent colloidal silica spheres as tracers for rotational diffusion studies. *Langmuir* **2000**, *16*, 6156.
(38) Verhaegh, N. A. M.; van Blaaderen, A. Dispersions of rhodamine-labeled silica spheres-synthesis, characterization, and fluorescence confocal scanning laser microscopy. *Langmuir* **1994**, *10*, 1427.
(39) Imhof, A.; Megens, M.; Engelberts, J. J.; de Lang, D. T. N.; Sprik, R.; Vos, W. L. Spectroscopy of fluorescein (FITC) dyed colloidal silica spheres. *J. Phys. Chem. B* **1999**, *103*, 1408.
(40) Makarova, O. V.; Ostafin, A. E.; Miyoshi, H.; Norris, J. R.; Meisel, D. Adsorption and encapsulation of fluorescent probes in nanoparticles. *J. Phys.Chem. B* **1999**, *103*, 9080.
(41) Dewar, P. J.; MacGillivray, T. F.; Crispo, S. M.; Smith-Palmer, T. Interactions of pyrene-labeled silica particles. *J. Colloid Interface Sci.* **2000**, *228*, 253.
(42) Bele, M.; Siiman, O.; Matijevic, E. Preparation and flow cytometry of uniform silica-fluorescent dye microspheres. *J. Colloid Interface Sci.* **2002**, *254*, 274.
(43) Larson, D. R.; Ow, H.; Vishwasrao, H. D.; Heikal, A. A.; Wiesner, U.; Webb, W. W. Silica nanoparticle architecture determines radiative properties of conjugated fluorophores. *Chem. Mater.* **2008**, *20*, 2677.
(44) Ow, H.; Larson, D. R.; Srivastava, M.; Baird, B. A.; Webb, W. W.; Wiesner, U. Bright and stable core-shell fluorescent silica nanoparticles. *Nano Lett.* **2005**, *5*, 113.
(45) Burns, A. A.; Vider, J.; Ow, H.; Herz, E.; Penate-Medina, O.; Baumgart, M.; Larson, S. M.; Wiesner, U.; Bradbury, M. Fluorescent silica nanoparticles with efficient urinary excretion for nanomedicine. *Nano Lett.* **2009**, *9*, 442.
(46) Ma, D.; Kell, A. J.; Tan, S.; Jakubek, Z. J.; Simard, B. Photophysical properties of dye-doped silica nanoparticles bearing different types of dye-silica interactions. *J. Phys. Chem. C* **2009**, *113*, 15974.
(47) Yokoi, T.; Sakamoto, Y.; Terasaki, O.; Kubota, Y.; Okubo, T.; Tatsumi, T. Periodic arrangement of silica nanospheres assisted by amino acids. *J. Am. Chem. Soc.* **2006**, *128*, 13664.
(48) Yokoi, T.; Iwama, M.; Watanabe, R.; Sakamoto, Y.; Terasaki, O.; Kubota, Y.; Kondo, J. N.; Okubo, T.; Tatsumi, T. Synthesis of well-ordered nanospheres with uniform mesopores assisted by basic amino acids. *Stud. Surf. Sci. Catal.* **2007**, *170*, 1774.
(49) Yokoi, T.; Wakabayashi, J.; Otsuka, Y.; Fan, W.; Iwama, M.; Watanabe, R.; Aramaki, K.; Shimojima, A.; Tatsumi, T.; Okubo, T. Mechanism of formation of uniform-sized silica nanospheres catalyzed by basic amino acids. *Chem. Mater.* **2009**, *21*, 3719.
(50) Bagwe, R. P.; Yang, C.; Hillard, L. R.; Tan, W. Optimization of dye-doped silica nanoparticles prepared using a reverse microemulsion method. *Langmuir* **2004**, *20*, 8336.
(51) Ha, S. W.; Camalier, C. E.; Beck, G. R.; Lee, J. K. New method to prepare very stable and biocompatible fluorescent silica nanoparticles. *Chem. Commun.* **2009**, *20*, 2881.
(52) Hartlen, K. D.; Athanasopoulos, A. P. T.; Kitaev, V. Facile preparation of highly monodisperse small silica spheres (15 to >200 nm) suitable for colloidal templating and formation of ordered arrays. *Langmuir* **2008**, *24*, 1714.
(53) Fyfe, C. A. *Solid State NMR for Chemists*; CFC Press: Guelph, Ontario, 1983.
(54) Sadasivan, S.; Dubey, A. K.; Li, Y. Z.; Rasmussen, D. H. Alcoholic solvent effect on silica synthesis - NMR and DLS investigation. *J. Sol—Gel Sci. Technol.* **1998**, *12*, 5.
(55) Harris, M. T.; Brunson, R. R.; Byers, C. H. The base-catalyzed-hydrolysis and condensation-reactions of dilute and concentrated TEOS solutions. *J. Non-Cryst. Solids* **1990**, *121*, 397.
(56) Green, D. L.; Jayasundara, S.; Lam, Y. F.; Harris, M. T. Chemical reaction kinetics leading to the first Stober silica nanoparticles - NMR and SAXS investigation. *J. Non-Cryst. Solids* **2003**, *315*, 166.
(57) Green, D. L.; Lin, J. S.; Lam, Y. F.; Hu, M. Z. C.; Schaefer, D. W.; Harris, M. T. Size, volume fraction, and nucleation of Stober silica nanoparticles. *J. Colloid Interface Sci.* **2003**, *266*, 346.
(58) Byers, C. H.; Harris, M. T.; Williams, D. F. Controlled microcrystalline growth-studies by dynamic laser-light-scattering methods. *Ind. Eng. Chem. Res.* **1987**, *26*, 1916.
(59) Peace, B. W.; Mayhan, K. G.; Montle, J. F. Polymers from the hydrolysis of tetraethoxysilane. *Polymer* **1973**, *14*, 420.
(60) Van Helden, A. K.; Jansen, J. W.; Vrij, A. Preparation and characterization of spherical monodisperse silica dispersions in non-aqueous solvents. *J. Colloid Interface Sci.* **1981**, *81*, 354.
(61) Bogush, G. H.; Tracy, M. A.; Zukoski, C. F. Preparation of monodisperse silica particles — control of size and mass fraction. *J. Non-Cryst. Solids* **1988**, *104*, 95.
(62) Rao, K. S.; Hami, K. E.; Kodaki, T.; Matsushige, K.; Makino, K. A novel method for synthesis of silica nanoparticles. *J. Colloid Interface Sci.* **2005**, *289*, 125.
(63) Ow, H.; Wiesner, U. U.S. Patent Publication Number: US2004101822, 2005.
(64) Jin, Y. H.; Lohstreter, S.; Pierce, D. T.; Parisien, J.; Wu, M.; Hall, C.; Zhao, J. X. J. Silica nanoparticles with continuously tunable sizes. Synthesis and size effects on cellular contrast Imaging. *Chem. Mater.* **2008**, *20*, 4411.